Reaction-Limited Island Nucleation in Molecular Beam Epitaxy of Compound Semiconductors

P. Kratzer and M. Scheffler

Fritz-Haber-Institut der Max-Planck-Gesellschaft, Faradayweg 4-6, D-14195 Berlin-Dahlem, Germany
(Received 18 February 2001; published 7 January 2002)

Kinetic Monte Carlo simulations on the basis of rates derived from density-functional calculations are used to investigate the atomic processes in molecular beam epitaxy of GaAs. This approach puts us in a position to describe island nucleation and growth in all relevant atomistic detail by bridging the gap in length and time scales between the mesoscopic scale of growth morphology and the atomic scale. We observe a nonmonotonic dependence of the island density on growth temperature related to a reversible surface reaction of As_2 with Ga adatoms.

Recent progress in experimental methods, in particular the use of scanning tunneling microscopy (STM), has made the elementary processes of crystal growth accessible to direct investigation. Frequently images of single-layer islands after deposition of a fraction of a monolayer (ML) of material are analyzed. This raises questions about the range of validity of nucleation theories successfully used to analyze metal epitaxy [1], e.g., if these theories also apply to the technologically important molecular beam epitaxy (MBE) of semiconductors. In MBE of compound materials, often one species is supplied in molecular form, and hence it may be necessary to weaken or even dissociate the molecular bond by a surface chemical reaction to incorporate the atoms of this species into the growing film. This is in contrast to the better understood epitaxy of metals, where surface diffusion and the aggregation of mobile surface species to an immobile stable nucleus are sometimes the only relevant processes that determine the growth morphology. In this case, simple power laws have been derived that describe the nucleation density of islands as a function of diffusivity and flux. Experimental data analysis has made extensive use of this power law scaling, even in the more complex case of semiconductor epitaxy (e.g., Refs. [2,3]). Therefore, a profound understanding of its range of validity is desirable.

In this Letter, we present a novel approach to semiconductor growth that enables us to combine a description of chemical bonding on the atomic level with investigations of the surface morphology at the large length and time scales that are characteristic for growth. This is achieved by performing kinetic Monte Carlo (kMC) simulations using rates derived from density-functional theory (DFT) calculations. We consider the use of techniques from statistical mechanics, such as kMC simulations, in combination with DFT calculations a necessary and important step towards a reliable description of growth, since it enables us to bridge the gap between an understanding of the microscopic physics and the resulting macroscopic phenomena.

As an example, we study the MBE growth of GaAs, the technologically most important of the III-V-compound semiconductors, from beams of atomic Ga and molecular As_2. Although it was realized a decade ago that

MBE growth of GaAs could be either diffusion limited or surface-reaction limited [4], modeling of growth in this system was mostly performed using a *single* "effective species" [5,6], in loose analogy to the paradigmatic case of metal epitaxy. Only recently some progress has been made with empirically derived growth models that treat both atomic species [7,8]. Here, we report simulations that address the interplay of more than 30 processes studied by DFT, none of which had been analyzed or understood in detail three years ago. The study reveals that only the analysis of the statistical interplay of such an ensemble of processes can identify the ones most relevant for growth.

We model island growth on the well-known $(2 \times 4)\beta2$ reconstruction of GaAs(001) that prevails under frequently used growth conditions. This As-rich surface reconstruction consists of pairs of As dimers, which alternate with "trenches" (two As dimers missing) running in the $[\bar{1}10]$ direction. Since growth on GaAs(001) involves a complex (2×4) reconstruction as well as the interaction of two very different species (Ga atoms and As_2 molecules), a large variety of processes with very different rates needs to be modeled. We use the energetics obtained from density-functional theory (DFT) calculations to determine these rates. Specifically, the calculations were performed using *ab initio* pseudopotentials and a plane-wave expansion of the electronic wave functions, employing the generalized gradient approximation for exchange and correlation [9,10]. Using transition-state theory, the rate law has the well-known Arrhenius form $\Gamma = \Gamma_0 \exp(-\Delta E/k_B T)$, with the activation energy ΔE given by the energy difference between the initial state and the transition state, as obtained from the DFT calculations. A common prefactor $\Gamma_0 = 10^{13}$ s^{-1} is used for all processes [11]. In order to assess the consequences of the calculated rates for nucleation and growth in different temperature regimes, we find it important to understand the interplay of the microscopic processes on time scales larger than milliseconds. kMC simulations offer an excellent tool to achieve this goal.

The state of the crystal during growth is represented on a three-dimensional lattice having the physically adequate zinc blende structure of GaAs. Arsenic atoms in the

topmost cation layer are dimerized along the $(\bar{1}10)$ direction, unless a Ga adatom is sitting between them. The starting surface is prepared in the thermodynamic ground state, the $(2 \times 4)\beta 2$ reconstruction of GaAs(001) with two top layer As dimers per unit cell. We introduce ubiquitous thermal disorder by placing three As dimers in some unit cells, corresponding to the β reconstruction, which is only $\Delta\gamma = 0.36$ eV per unit cell higher in energy than $\beta 2$. The β unit cells are selected randomly with a probability $\exp(-\Delta\gamma/k_B T)$ prior to starting the simulation.

The selection of the microscopic processes considered in the simulation is guided both by experimental knowledge and previous theoretical studies. Experiments suggest that arsenic and gallium behave quite differently on the GaAs(001) surface. While Ga atoms adsorb with unit sticking probability, As$_2$ molecules find sufficiently strong binding sites only after Ga has been deposited [12,13]. Previous calculations using density-functional theory indeed found a barrierless adsorption pathway for the As$_2$ molecule close to Ga adatoms [14], while interaction of the As$_2$ with the pristine surface proceeds through weak molecular adsorption at several sites. We take the effect of this previously described [13,14] mobile molecular precursor into account by working with a renormalized As$_2$ flux $F^*_{\mathrm{As_2}} = p^*/\sqrt{2\pi m_{\mathrm{As_2}} k_B T}$. For the simulations, we use an estimated value of $p^* = 8.5 \times 10^{-7}$ bar [15]. Under these conditions, the As$_2$ molecules *in the precursor* probe each surface site with a rate of 100 s^{-1}. Since our DFT calculations found no evidence for a dissociative adsorption pathway of As$_2$, we assume that the surface mobility of arsenic is mainly due to the precursor state, while any contribution of an atomic As surface species is neglected. Mobility of single Ga adatoms [16], however, is essential for growth, because suitable sites for As$_2$ incorporation into a new layer are created only after several Ga adatoms have arranged themselves in adjacent sites. In the following we describe the processes included in the present simulations in detail.

(i) Ga adsorption: Ga atoms are deposited randomly with a flux of 0.1 ML/s typical for MBE.

(ii) Ga surface diffusion: Because of the surface reconstruction, the rates for hopping of Ga adatoms are highly site specific. We include 10 different hopping processes for an isolated Ga adatom in our model (9 of them are shown in Fig. 1). Ga diffusion is anisotropic with an activation energy of 0.8 eV in the [110] direction and 0.7 eV in the $[\bar{1}10]$ direction, along the trenches [17]. We note that the strongest adsorption sites for Ga are located within As surface dimers [16]. During the simulation, rates from an externally supplied list are assigned to the hopping processes on the basis of logical attributes describing the local environment of the moving atom. For Ga atoms with one or two Ga neighbors, hopping rates are modified by adding the binding energy of these configurations, as obtained in DFT [10], to the barrier for the corresponding jump of the isolated atom.
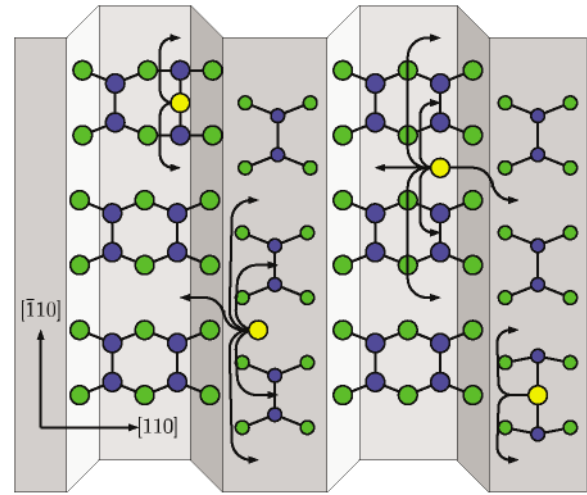

FIG. 1 (color). Top view of the "trench-and-hill" structure of the GaAs(001)$\beta 2(2 \times 4)$ surface. Arrows indicate elementary hopping processes of Ga adatoms (yellow). Ga and As atoms of the substrate are shown in green and dark blue.

(iii) Ga incorporation: If a Ga adatom reaches a strongly bound configuration, it is considered incorporated into the crystal and is no longer available for diffusion. The DFT calculations show that this occurs if it forms a dimer with a Ga neighbor in [110] direction in the top layer; if an As dimer is adsorbed above it; if it sits in the interior of a string of Ga atoms in the trench; if it sits between an As dimer and a bulklike coordinated As atom, as realized at steps running in [110] direction.

(iv) As$_2$ adsorption: Previous DFT calculations [14] have shown that As$_2$ molecules can adsorb without being dissociated, but rather become incorporated as an As surface dimer, with the dimer axis oriented along $[\bar{1}10]$. Generalizing from numerous calculations for different adsorption sites, we find that the binding energy of As$_2$ correlates with the number of bonds to Ga atoms that the As$_2$ molecule can form at a particular site. In the simulations, we include As$_2$ adsorption on those lattice sites where it can form three or four bonds to Ga atoms. A pair of free sites in the arsenic sublattice is eligible for As$_2$ adsorption if it is surrounded by three or four Ga atoms with one dangling bond each, denoted by Ga*, on the cation sublattice. Since there are Ga atoms with dangling bonds in both sidewalls of the trench, a single additional Ga adatom is sufficient to create an adsorption site for As$_2$ in the trench, while this requires at least three adatoms in adjacent sites in the top layer. Thus As$_2$ adsorption in the trench is more likely to occur in the early stages of growth. However, our previous DFT calculations [10] have shown that adsorption of two As dimers side-by-side in the trench would result in a weakly bound As dimer. In the simulations, the instability of this geometry is taken into account: Side-by-side adsorption of As$_2$ molecules in the trench is enabled only after at least one Ga atom adsorbed next to the trench enhances again the binding energy of As$_2$ in the trench [18].

Thus the trenches are leveled out only after island growth in the new layer has started.

(v) As_2 desorption: There are three As_2 desorption events with different rates in our model, depending on the chemical environment the As_2 is bonded to. These are desorption of As_2 from sites where it had three bonds to Ga atoms ($\Delta E = 1.9$ eV); desorption of As_2 from sites where it had four bonds to Ga atoms, but was misaligned with an adjacent As dimer row ($\Delta E = 1.9$ eV); desorption of one of the outermost As_2 from a row of three adjacent As surface dimers (local β structure, $\Delta E = 2.4$ eV). In this case, the desorbing As dimer had four bonds to Ga. Despite the high barrier for this process, it is necessary to include it to make it possible for the β structure to decay to the ground state of the surface, which is the $\beta 2$ structure.

The kMC simulations show that island growth at $T = 700$ K is initiated by an As_2 molecule adsorbing at a Ga adatom in a trench site. From this starting point, growth initially proceeds by attachment of more Ga atoms and further As_2 adsorption along the trenches (Fig. 2a). Incorporation of two Ga atoms and one As_2 in one unit cell induces locally the β reconstruction that acts as a long-lived intermediate state. A similar "pair-wise addition of Ga atoms" was identified earlier [20] as an essential requirement for understanding the growth kinetics on the GaAs(001) surface. In the regions of the surface where growth in the trenches has been initiated, we observe a preference for island formation in a new layer. The incorporation of material in the new layer starts from strongly bound Ga dimers (Fig. 2b), which line up along the $[\bar{1}10]$ direction and later become covered by arsenic (Fig. 2c).

The results are analyzed quantitatively by studying the island density as a function of growth temperature (Fig. 3). For typical pressures in MBE, the $\beta 2$ reconstruction is observed between $T = 800$ and 850 K. Yet we decided to perform simulations over a wider temperature range, from 500 up to 900 K. While DFT calculations can reliably predict the relative sequence of barrier heights, absolute barrier heights are not available yet with an accuracy better than ± 0.1 eV. Because of the resulting uncertainty in the temperature scale, we prefer to do simulations in a wider temperature range than experimentally accessible.

An important feature of the submonolayer growth regime is the saturation of the island density after a certain amount of material has been deposited, as evidenced in Fig. 3a. Depending on temperature, this situation is reached in our simulations after deposition of 0.1–0.15 ML, in agreement with previous experiments [21]. Figure 3b shows a decrease of the saturation island density when the substrate temperature is increased from 500 to 600 K, in accordance with standard nucleation theory. However, the island density remains nearly constant above 600 K, and even rises again for $T > 800$ K. The reason for the sharp rise above 800 K becomes clear when one considers the balance of material flow of As at the growing surface. As_2 attaches to sites where either three or four Ga dangling bonds are available. An analysis of the simulation data shows that at low temperatures and sufficiently high As_2 partial pressures, supply is dominated by the complexes initially formed from As_2 with three Ga surface atoms, Ga-As-As-Ga_2. At higher temperature, these complexes become unstable against As_2 desorption, and only a small fraction of them can stabilize by capturing a Ga adatom and forming the more long-lived Ga_2-As-As-Ga_2 complex. Because of the instability of the Ga-As-As-Ga_2 intermediate, attachment of diffusing Ga adatoms to island edges becomes reversible. This, in turn, leads to a higher density of mobile Ga adatoms, a higher nucleation rate of new islands, and thus to the observed rise of the saturation island density at temperatures above 800 K.

At $T \geq 850$ K, As_2 adsorption and desorption become fully reversible. As a consequence, we observe that structures grown in the trenches can dissolve again, and their material is transferred to islands in the new layer. Thus, the trench structures can no longer be considered as stable nuclei for growth. However, we observe that the growth of an island is still triggered in the trench, but proceeds quickly into the new layer. Both effects give rise to a growth morphology where trenches are filled if and only if they are part
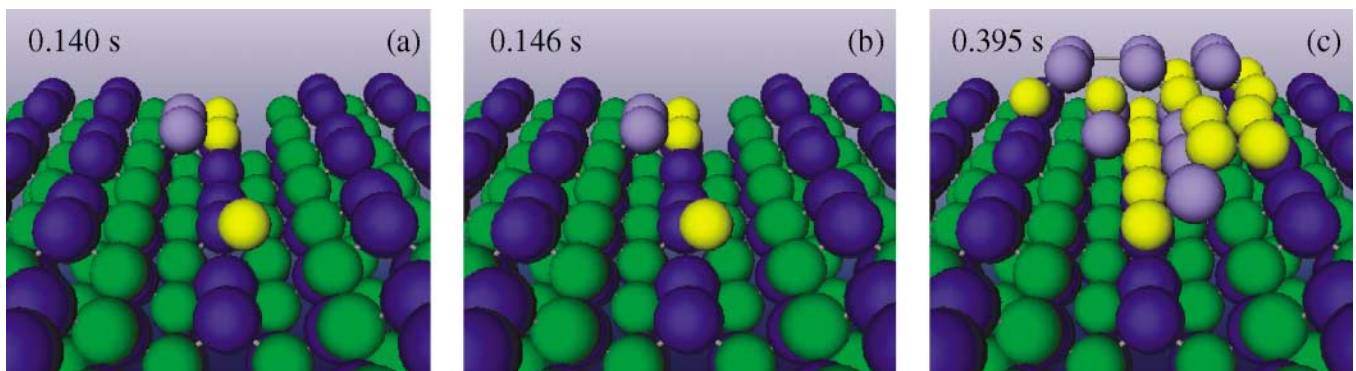

FIG. 2 (color). Snapshots of a movie [19] of MBE growth for 1 sec at $T = 700$ K, Ga flux 0.1 ML/sec. Ga and As atoms of the substrate are shown in green and dark blue, Ga adatoms in yellow, and As ad-dimers in light blue.
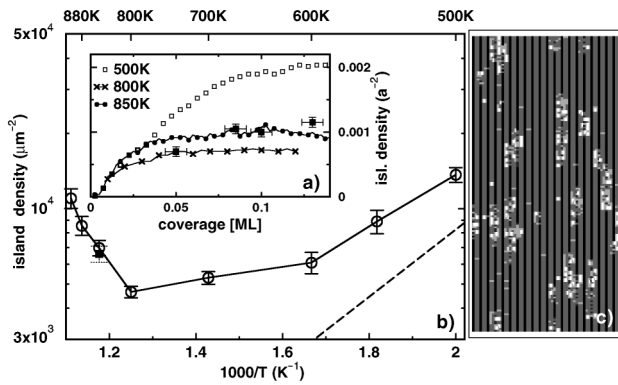
FIG. 3. (a) Time evolution of the island densities per surface unit cell $a^2 = 16$ Å^2 at various temperatures, compared to experimental data at $T = 850$ K from Ref. [21] (filled squares). (b) Saturation island density as a function of the inverse growth temperature (open circles). All simulations were performed with a Ga flux of 0.1 ML/sec and an effective As$_2$ pressure of $p^* = 8.5 \times 10^{-7}$ bar. Experimental data from Ref. [22] are shown as a filled square. The dashed line shows the prediction of a frequently applied scaling law for a critical nucleus size of one and the Ga diffusion constant along [110], $D = D_0 \exp(-0.8 \text{ eV}/k_B T)$. (c) Island morphology in a simulation area of 80×160 a^2 after deposition of 0.11 ML GaAs at $T = 900$ K. The trenches and rows of As-dimer pairs of the $\beta 2$ reconstruction are marked in black and dark gray, freshly deposited material in light gray, and As dimers grown in the new layer in white.

of an island that also extends to the new layer, and mostly empty otherwise (Fig. 3c), consistent with STM images recorded after growth of 0.1 ML followed by fast cooling to room temperature [22]. We note that previous analysis of STM images using a growth model with adjustable parameters had come to different conclusions about the location where island growth starts. The differences could at least partly be due to different growth conditions modeled in Ref. [7] and in the present simulation. We point out that in our simulations the distribution of Ga adatoms on the surface is driven out of equilibrium by a substantial arsenic flux, while a population of Ga adatoms close to equilibrium would eventually condense into Ga ad dimers in the top layer, similar to the assumptions made in Ref. [7]. Here we stress that both simulations predict statistical quantities, such as island densities, in good agreement with STM experiments. While the experiments find an island density of 6600 μm^{-2} at $T = 850$ K [22,23], our simulations yield ~ 7000 μm^{-2}.

In summary, the present study demonstrates the feasibility of first-principles growth simulations even for a complex compound material. It reveals that the power law scaling for the island density that has proven useful in data analysis for metal islands cannot describe the temperature dependence of the island density in MBE of a compound semiconductor. One reason for the deviations is the instability of Ga-As-As-Ga$_2$ complexes at elevated tempera-

tures. The temperature window frequently used by MBE crystal growers is a compromise between high Ga adatom mobility and a sufficient lifetime of these complexes that allows them to grow films from a low island density.

[1] J. A. Venables, *Surface and Thin Film Processes* (Cambridge University Press, Cambridge, United Kingdom, 2000).

[2] Y.-W. Mo, J. Kleiner, M. B. Webb, and M. G. Lagally, Phys. Rev. Lett. **66**, 1998 (1991); Surf. Sci. **268**, 275 (1992).

[3] V. P. LaBella et al., J. Vac. Sci. Technol. A **18**, 1526 (2000).

[4] S. V. Ghaisas and A. Madhukar, Phys. Rev. Lett. **56**, 1066 (1986).

[5] T. Shitara et al., Phys. Rev. B **46**, 6815 (1992).

[6] P. Smilauer, M. R. Wilby, and D. D. Vvedensky, Phys. Rev. B **47**, 4119 (1993).

[7] M. Itoh et al., Phys. Rev. Lett. **81**, 633 (1998).

[8] A. Ishii and T. Kawamura, Surf. Sci. **436**, 38 (1999).

[9] J. P. Perdew, K. Burke, and M. Ernzerhof, Phys. Rev. Lett. **77**, 3865 (1996).

[10] P. Kratzer, C. G. Morgan, and M. Scheffler, Phys. Rev. B **59**, 15 246 (1999).

[11] Within the framework of transition state theory, it is possible to determine prefactors from first principles. For Ga diffusion on GaAs(001), previous calculations have found prefactors of the order of 10^{12} to 10^{13} sec^{-1} for all hopping processes considered [16]. Thus, the effect of possible prefactor variations is expected to be small.

[12] C. T. Foxon and B. A. Joyce, Surf. Sci. **64**, 293 (1977).

[13] E. S. Tok, J. H. Neave, J. Zhang, B. A. Joyce, and T. S. Jones, Surf. Sci. **374**, 397 (1997).

[14] C. G. Morgan, P. Kratzer, and M. Scheffler, Phys. Rev. Lett. **82**, 4886 (1999).

[15] The effective pressure p^* relates to the applied flux F of As$_2$ through $p^* = F\sqrt{2\pi m k_B T} \exp[(E_B/k_B T) - 1]$, where $E_B \sim 0.3$ eV is the binding energy of the precursor.

[16] A. Kley, P. Ruggerone, and M. Scheffler, Phys. Rev. Lett. **79**, 5278 (1997).

[17] Numerical differences to Ref. [16] result both from the use of thicker slabs and a different DFT functional [9].

[18] K. Shiraishi and T. Ito, Phys. Rev. B **57**, 6301 (1998).

[19] See AIP Document No. EPAPS: E-PRLTAO-87-031152 for a movie corresponding to the snapshots of Fig. 2. This document may be retrieved via the EPAPS homepage (http://www.aip.org/pubservs/epaps.html) or from ftp.aip.org in the directory /epaps/. See the EPAPS homepage for more information.

[20] B. A. Joyce et al., Appl. Surf. Sci. **132**, 357 (1998).

[21] M. Itoh et al., Surf. Sci. **464**, 200 (2000).

[22] G. R. Bell, M. Itoh, T. S. Jones, and B. A. Joyce, Surf. Sci. **423**, L280 (1999).

[23] B. A. Joyce et al., J. Cryst. Growth **201/202**, 106 (1999).